

A Raman study of the charge-density-wave state in $A_{0.3}MoO_3$ ($A = K, Rb$)

D. M. Sagar, D. Fausti, S. Yue, Christine A. Kuntscher, Sander van Smaalen, P. H. M. van Loosdrecht

Angaben zur Veröffentlichung / Publication details:

Sagar, D. M., D. Fausti, S. Yue, Christine A. Kuntscher, Sander van Smaalen, and P. H. M. van Loosdrecht. 2008. "A Raman study of the charge-density-wave state in $A_{0.3}MoO_3$ ($A = K, Rb$)."
New Journal of Physics 10 (2): 023043.
<https://doi.org/10.1088/1367-2630/10/2/023043>.

A Raman study of the charge-density-wave state in $A_{0.3}\text{MoO}_3$ (A = K, Rb)

To cite this article: D M Sagar *et al* 2008 *New J. Phys.* **10** 023043

View the [article online](#) for updates and enhancements.

Recent citations

- [Phase-channel dynamics reveal the role of impurities and screening in a quasi-one-dimensional charge-density wave system](#)
M. D. Thomson *et al*
- [Dynamical Stability Limit for the Charge Density Wave in \$\text{K}_{0.3}\text{MoO}_3\$](#)
R. Mankowsky *et al*
- [Charge density wave phase transition on the surface of electrostatically doped multilayer graphene](#)
Gen Long *et al*



IOP | ebooks™

Bringing you innovative digital publishing with leading voices to create your essential collection of books in STEM research.

Start exploring the collection - download the first chapter of every title for free.

A Raman study of the charge-density-wave state in $A_{0.3}MoO_3$ ($A = K, Rb$)

D M Sagar^{1,4}, D Fausti¹, S Yue², C A Kuntscher^{2,5},
S van Smaalen³ and P H M van Loosdrecht^{1,6}

¹ Zernike Institute for Advanced Materials, University of Groningen,
9747 AG Groningen, The Netherlands

² Physikalisches Institut, Universität Stuttgart, Pfaffenwaldring 57,
70550 Stuttgart, Germany

³ Laboratory of Crystallography, University of Bayreuth,
95440 Bayreuth, Germany

E-mail: p.h.m.van.loosdrecht@rug.nl

New Journal of Physics **10** (2008) 023043 (11pp)

Received 22 December 2007

Published 26 February 2008

Online at <http://www.njp.org/>

doi:10.1088/1367-2630/10/2/023043

Abstract. We report a comparative Raman spectroscopic study of the quasi-one-dimensional charge-density-wave (CDW) systems $A_{0.3}MoO_3$ ($A = K, Rb$). Temperature- and polarization-dependent experiments reveal charge-coupled vibrational Raman features. The strongly temperature-dependent collective amplitudon modes in the two materials differ by about 3 cm^{-1} , thus revealing the role of the alkali atom. We discuss the observed vibrational features in terms of the CDW ground state accompanied by a change in the crystal symmetry. A frequency-kink in some modes seen in $K_{0.3}MoO_3$ between $T = 80$ and 100 K supports the first-order lock-in transition, unlike the case of $Rb_{0.3}MoO_3$. The unusually sharp Raman lines (limited by the instrumental response) at very low temperatures and their temperature evolution suggests that the decay of the low-energy phonons is strongly influenced by the presence of the temperature-dependent CDW gap.

⁴ Present address: Department of Chemistry, University of McGill, 801 Sherbrooke St. West, Montreal, QC, H3A 2K6, Canada.

⁵ Present address: Experimentalphysik 2, Universität Augsburg, 86135 Augsburg, Germany.

⁶ Author to whom any correspondence should be addressed.

Contents

1. Introduction	2
2. Experimental details	3
3. Raman spectra of $K_{0.3}MoO_3$ and $Rb_{0.3}MoO_3$ above and below T_{CDW}	3
4. Temperature-dependent Raman spectra	6
5. Summary	9
Acknowledgments	10
References	10

1. Introduction

Quasi-one-dimensional (1D) metals are interesting materials because of their tendency to undergo a phase transition inevitably due to an inherent instability called the Peierls instability [1]. This instability, originating from the electron–phonon interaction, leads to a metal–insulator transition at reduced temperatures, where the insulating state may be characterized by a lattice deformation in conjunction with a charge modulation and the opening of a single-particle excitation gap in the electronic spectrum [2]. One of the striking features of these materials is their unusual non-linear electrical conduction properties [3]–[5], which arises from the collective motion of the charge-density-wave (CDW). Along with the conventional single-particle excitations, these materials also have collective excitations, namely, amplitudons and phasons, which dominate the low-energy physical properties [3]. The Raman⁷ active collective amplitudon mode, i.e. the transverse oscillation of the amplitude of the coupled charge–lattice wave, has been observed by various researchers [8, 9].

The $A_{0.3}MoO_3$ ($A = \text{any alkali metal}$) blue bronze is one of the best-known quasi-1D materials that undergo a CDW transition [3, 8, 10] via the Peierls channel. The first evidence of the CDW transition in $K_{0.3}MoO_3$ by Raman measurements came from the experiments of Travaglini *et al* [8]. In this paper, a mode around 50 cm^{-1} was observed at temperatures below $T_{CDW} = 180 \text{ K}$ that showed a strong temperature dependence of, in particular, its frequency when the temperature approached T_{CDW} from below. As it was also found that this is a fully symmetric (A_g -mode) breathing mode, it was assigned to the amplitude oscillation of the CDW. Further evidence came from the observation that the line width tended to diverge as the T_{CDW} was approached from below. This anomalous behaviour of the line width could be due to the fluctuation effects that become pronounced in the vicinity of the phase transition. The mean-field theory of a generalized second-order phase transition predicts that, due to a temperature-dependent order parameter, the frequency (and the amplitude) of the soft mode tends to zero as the temperature approaches T_{CDW} [2]. However, in the study of Travaglini *et al* [8], the softening of the amplitudon mode with increasing temperature was found to be incomplete. The observed softening of only $\sim 13\%$ was ascribed to 3D correlations. The 3D correlations are nothing but the long-range Coulomb interaction between density-modulated electrons, which might effectively screen the electron–phonon interaction [11, 12], thereby reducing the expected complete mode-softening. The effects of strong local electron–electron interactions lead to both dynamical and

⁷ For a general discussion on Raman scattering in solids, see [6]; for a recent review of the applications of Raman spectroscopy to correlated electron systems, see [7].

static screening processes dressing the electron–phonon coupling. These screening effects are thought to be a generic feature of strongly correlated electron systems.

Recently, a Raman study of the anomalous profile of the amplitudon mode in $\text{K}_{0.3}\text{MoO}_3$ was reported [13] in which, for temperatures below 100 K, the amplitudon mode showed an anomalous ‘fin’-like profile toward the Stokes side of its central frequency. This was interpreted as a splitting of the amplitudon mode into two or more closely spaced harmonic oscillator-type modes. The splitting was claimed to be due to a strong perturbation of the CDW by impurity potentials. At very low temperatures where there are practically no thermally excited electrons, the impurity potentials remain unscreened, leading to a spatial variation of the CDW amplitude and a splitting of the amplitudon mode.

The present paper revisits the vibrational and electronic excitations in the blue bronzes through a comparative study of $\text{Rb}_{0.3}\text{MoO}_3$ and $\text{K}_{0.3}\text{MoO}_3$ in order to examine the behaviour of the amplitudon mode in both the compounds together with a detailed temperature- and polarization-dependent study of the low-energy phonons.

2. Experimental details

At room temperature, the $\text{K}_{0.3}\text{MoO}_3$ and $\text{Rb}_{0.3}\text{MoO}_3$ bronzes crystallize in the monoclinic $C2/m$ space group [14] with lattice constants $a = 16.23 \text{ \AA}$, $b = 7.5502 \text{ \AA}$, $c = 9.8 \text{ \AA}$ and $\beta = 94.89^\circ$ for $\text{K}_{0.3}\text{MoO}_3$ and $a = 16.36 \text{ \AA}$, $b = 7.555 \text{ \AA}$, $c = 10.094 \text{ \AA}$ and $\beta = 93.87^\circ$ for $\text{Rb}_{0.3}\text{MoO}_3$. There are 20 formula units per unit cell. The structure is built up of edge- and corner-sharing clusters of ten strongly distorted MoO_6 octahedra stacked along the [010] direction. These clusters form layers in the (102) planes, which are separated by the alkali ions.

At the CDW transition temperature, the structure transforms into an incommensurately modulated structure with a temperature-dependent incommensurate wavevector \mathbf{q}_{ic} close to (but not equal to) $0.25\mathbf{b}^* + \frac{1}{2}\mathbf{c}^*$ [15, 16]. At low temperatures ($T < 100 \text{ K}$), the incommensurate wavevector becomes temperature-independent, even though this does not seem to correspond to a lock-in transition, that is, the modulation remains incommensurate [16].

$\text{K}_{0.3}\text{MoO}_3$ and $\text{Rb}_{0.3}\text{MoO}_3$ single crystals with a typical size of $5 \times 3 \times 0.5 \text{ mm}^3$ were prepared by the temperature gradient flux method [17]. After polishing, samples were mounted in an optical flow cryostat (temperature stabilization better than 0.1 K) and backscattering Raman spectra were recorded (frequency resolution $\sim 2 \text{ cm}^{-1}$) by using a triple grating monochromator in the subtractive mode equipped with a liquid-nitrogen-cooled CCD detector. A solid-state diode-pumped, frequency-doubled Nd : YVO₄ laser system was used as the excitation source (wavelength 532 nm, and spot size $10 \mu\text{m}$). The power density was kept below 100 W cm^{-2} in order to minimize the heating effects. The polarization was controlled on both the incoming and outgoing beams, giving access to all the polarizations allowed for by the backscattering configuration. In general, both parallel ((xx) , where x is in the [20-1] direction, and (bb) in Porto notation) and perpendicular polarizations have been measured. The perpendicular spectra did not yield an appreciable scattering intensity and will therefore not be discussed here.

3. Raman spectra of $\text{K}_{0.3}\text{MoO}_3$ and $\text{Rb}_{0.3}\text{MoO}_3$ above and below T_{CDW}

Figure 1 shows the Raman spectra of $\text{K}_{0.3}\text{MoO}_3$ and $\text{Rb}_{0.3}\text{MoO}_3$ above T_{CDW} for (bb) and (xx) polarizations. Above T_{CDW} the Raman spectra of $\text{K}_{0.3}\text{MoO}_3$ and $\text{Rb}_{0.3}\text{MoO}_3$ show very similar

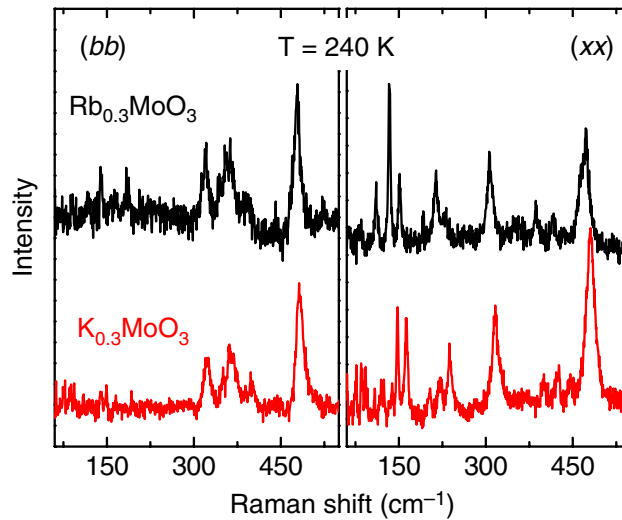


Figure 1. Polarized (*bb*) and (*xx*) Raman spectra of $\text{K}_{0.3}\text{MoO}_3$ and $\text{Rb}_{0.3}\text{MoO}_3$ above T_{CDW} . Spectra have been given an offset for clarity.

Raman vibrational features. Only a few modes are observed in the (*bb*) spectra (figure 1, left panel), since here the polarizations are along the metallic direction. There is a strong mode near 475 cm^{-1} , a triplet with frequencies near 320 , 365 and 400 cm^{-1} and some weaker modes below 200 cm^{-1} . The symmetric (A_g) modes above 300 cm^{-1} originate from bending vibrations of the MoO_6 units, as has already been noted in previous studies on blue bronzes [18, 19], and are consistent with the interpretation of the Raman spectra of pure MoO_3 [20]. There are quite a few different modes originating from the MoO_6 units, due to the large distortion of the MoO_6 ‘octahedra’; the metal–oxygen distances in blue bronzes typically range from 1.7 to 2.3 \AA [15]. The Mo–O stretching modes appear at higher frequencies (between 900 and 1000 cm^{-1}) [20] as reported by Nishio and Kakihana [21] and Massa [22]. In general, the frequencies for the modes observed in $\text{Rb}_{0.3}\text{MoO}_3$ are somewhat lower than the corresponding modes in $\text{K}_{0.3}\text{MoO}_3$. This is consistent with the fact that $\text{Rb}_{0.3}\text{MoO}_3$ has slightly larger lattice constants in the *a*- and *c*-directions [15, 23] resulting from the larger ionic radius of the rubidium ion. A small variance in the various Mo–O distances between $\text{K}_{0.3}\text{MoO}_3$ and $\text{Rb}_{0.3}\text{MoO}_3$ has also been observed in the study of Schutte and de Boer [15].

The right panel of figure 1 shows the Raman spectra of $\text{K}_{0.3}\text{MoO}_3$ and $\text{Rb}_{0.3}\text{MoO}_3$ ($T > T_{\text{CDW}}$) for the polarizations of the incident and scattered light in the *x*-direction, i.e. perpendicular to the metallic direction. As expected, the scattering efficiency in this direction is substantially higher than in the metallic direction, and many more modes are observed. In both $\text{Rb}_{0.3}\text{MoO}_3$ and $\text{K}_{0.3}\text{MoO}_3$, there are about 20 modes that are resolved in the present experiment. Again, the overall spectra are qualitatively very similar and many of the $\text{Rb}_{0.3}\text{MoO}_3$ vibrational modes are shifted toward a slightly lower frequency in comparison to the $\text{K}_{0.3}\text{MoO}_3$ modes. For instance, the triplet near 150 cm^{-1} in the $\text{K}_{0.3}\text{MoO}_3$ bronze is found some 10 – 15 cm^{-1} lower in energy in the $\text{Rb}_{0.3}\text{MoO}_3$ spectra, and the 480 cm^{-1} $\text{K}_{0.3}\text{MoO}_3$ mode is observed at 473 cm^{-1} in $\text{Rb}_{0.3}\text{MoO}_3$.

Finally, note that group theory predicts 71 A_g modes for the high-temperature phase of the bronzes. The experimental spectra, however, reveal only 35 modes. The ‘missing’ modes most likely result from accidental degeneracies and from weak intensity and/or screening, in

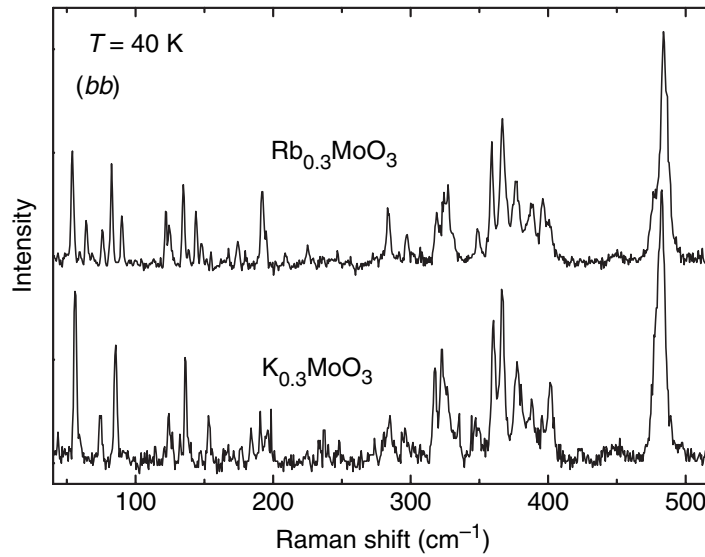


Figure 2. (*bb*) Polarized Raman spectra of $\text{K}_{0.3}\text{MoO}_3$ and $\text{Rb}_{0.3}\text{MoO}_3$ below T_{CDW} . Spectra have been given an offset for clarity.

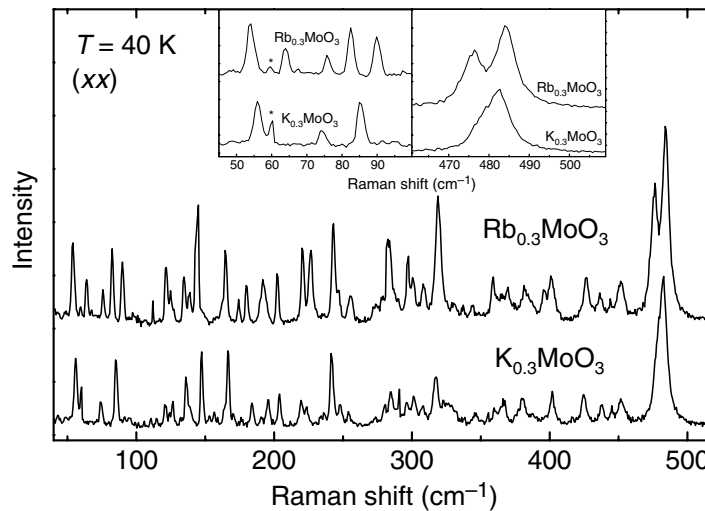


Figure 3. The (*xx*) polarized Raman spectra of $\text{K}_{0.3}\text{MoO}_3$ and $\text{Rb}_{0.3}\text{MoO}_3$ below T_{CDW} . Spectra have been given an offset for clarity. The insets show details of the splitting of some of the modes. The peak at 60 cm^{-1} marked by an asterisk is an experimental artefact originating from the air.

particular in the metallic direction. For the predicted $55 B_g$ modes (*xb* geometry) the intensity is too weak to be detected in the present experiments.

The low-temperature phase shows a much richer spectrum than the high-temperature one (see figures 2 and 3), showing many quite narrow Raman modes. The (*bb*)-polarized low-temperature spectra (figure 2) exhibit 32 distinct modes for the $\text{K}_{0.3}\text{MoO}_3$ compound, and 42 in the $\text{Rb}_{0.3}\text{MoO}_3$ compound. For the (*xx*) polarization (figure 3), the number of observed modes is

38 and 44 for $\text{K}_{0.3}\text{MoO}_3$ and $\text{Rb}_{0.3}\text{MoO}_3$, respectively. Again, the spectra for the two compounds are quite similar. The main difference is in the number of observed modes, which seems to originate from an additional splitting of modes in the $\text{Rb}_{0.3}\text{MoO}_3$ case. For instance, the doublet observed near 75 cm^{-1} in $\text{K}_{0.3}\text{MoO}_3$ is seen as a triplet (see also the left inset of figure 3). We note that, in a previous Raman study [22], a band near 80 cm^{-1} was observed in $\text{Rb}_{0.3}\text{MoO}_3$ that was ascribed to a zone-folded mode arising from the folding of the original Brillouin-zone due to CDW transition. The picture of zone-folding-active phonons is corroborated by previous neutron scattering studies by Pouget *et al* [24] in which a flat dispersion-less phonon branch was observed. In the present study, three modes are observed in the $\text{K}_{0.3}\text{MoO}_3$ compound in the $40\text{--}100\text{ cm}^{-1}$ region, and five in the $\text{Rb}_{0.3}\text{MoO}_3$ compound. As discussed in section 4, the lowest modes at 56 cm^{-1} ($\text{K}_{0.3}\text{MoO}_3$) and 53 cm^{-1} ($\text{Rb}_{0.3}\text{MoO}_3$) are the amplitudon mode of the CDW. Note that only a single mode is observed here, and no evidence is found for the ‘fin’-like structure as discussed by Nishio and Kakihana [13]. Also the Mo–O bending modes show an additional splitting in the $\text{Rb}_{0.3}\text{MoO}_3$ compound, which is exemplified by the right inset of figure 3 for the 480 cm^{-1} mode. As a general rule, the splitting of Raman modes occurs mainly due to two mechanisms. The first one occurs when a static distortion transforms equivalent atomic positions to inequivalent ones [25]. A second mechanism is the correlation field or Davydov [25]–[27] splitting that occurs due to coupling of vibrations of molecular units at different equivalent sites in the unit cell, and is sensitive to transitions involving multiplication of the unit cell size (like for instance the Peierls distortion). The incommensurate nature of the blue bronzes may also activate vibrational modes in Raman spectra [28]. Modes with wavevector $\mathbf{k} = n\mathbf{q}$ become active in the incommensurate phase, where \mathbf{q} is the incommensurate modulation vector, and their scattering strength depends strongly on the modulation amplitude.

4. Temperature-dependent Raman spectra

The temperature dependence of the low-frequency modes of both compounds is depicted in figure 4 for a few selected temperatures. As mentioned before, in $\text{K}_{0.3}\text{MoO}_3$ there are only two clear phonons observed in this region at 74 and 85 cm^{-1} , whereas the $\text{Rb}_{0.3}\text{MoO}_3$ compound shows four phonon modes in this region centred at 64 , 75 , 83 and 90 cm^{-1} . This, as well as the previously noted additional splitting in some of the high-frequency modes in $\text{Rb}_{0.3}\text{MoO}_3$, strongly indicates that the low-temperature structures of the two compounds are not completely identical. In general, it is thought that the crystal structures of $\text{Rb}_{0.3}\text{MoO}_3$ and $\text{K}_{0.3}\text{MoO}_3$ are, apart from the unit cell dimensions, the same [14, 15, 22]. The only relevant small difference lies in the incommensurate modulation. Both structures have their incommensurate modulation along the \mathbf{b}^* -direction. The amplitude of the modulation, however, is found to be substantially larger for the $\text{Rb}_{0.3}\text{MoO}_3$ compound [15]. Therefore, we tentatively conclude that the observation of a larger number of modes in $\text{Rb}_{0.3}\text{MoO}_3$, as compared to $\text{K}_{0.3}\text{MoO}_3$, is due to the larger displacement amplitude of the incommensurate modulation in the low-temperature phase.

Upon decreasing the temperature, the modes in $\text{Rb}_{0.3}\text{MoO}_3$ show a continuous behaviour, and no further indications of a possible additional phase transition are found. This is in contrast to the situation in $\text{K}_{0.3}\text{MoO}_3$. Upon lowering the temperature, some of the modes show an abrupt change in their energy in the range between 80 and 100 K . This is exemplified in figure 5. Clearly, some of the modes show a discontinuous shift to a higher energy of a few wavenumbers,

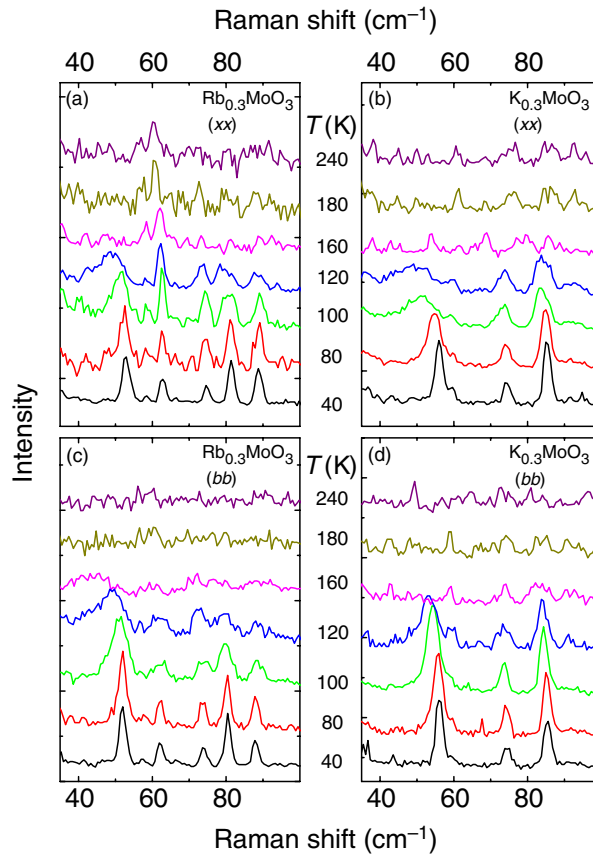


Figure 4. Polarized Raman spectra of $\text{K}_{0.3}\text{MoO}_3$ and $\text{Rb}_{0.3}\text{MoO}_3$ at selected temperatures. (a) and (b) The (xx) spectra; (c) and (d) the (bb) spectra. The spectra have been given an offset for clarity.

indicating a phase transition. It should be noted that not all modes exhibit the frequency-‘kink’, as can for instance be seen for the 75 cm^{-1} mode in figure 5. In general, a temperature-dependent frequency-jump is a signature of a first-order transition. In the present case, it could be due to a lock-in transition to a commensurate state. However, the low-temperature phase of $\text{K}_{0.3}\text{MoO}_3$ has been studied in quite some detail, and temperature-dependent neutron scattering experiments [16] failed to show a lock-in transition in $\text{K}_{0.3}\text{MoO}_3$. It was found that the incommensurate wavevector is strongly temperature-dependent down to $T = 100\text{ K}$. Below this temperature the wavevector becomes temperature-independent, but remains incommensurate. Still, the present study strongly indicates that there is indeed a first-order phase transition in $\text{K}_{0.3}\text{MoO}_3$ below 100 K .

The most striking feature of the low-frequency spectra is the appearance of the amplitudon in both compounds, which shows a softening and broadening upon approaching the phase transition (see figure 4). The low-temperature frequencies of these modes are 56 cm^{-1} in the $\text{K}_{0.3}\text{MoO}_3$ compound and 53 cm^{-1} in $\text{Rb}_{0.3}\text{MoO}_3$. The interpretation of these modes as amplitudon modes is consistent with the previous neutron study by Pouget *et al* [24] and Raman scattering studies by Travaglini *et al* [8] and Massa [22]. Recently this mode has also been observed in $\text{K}_{0.3}\text{MoO}_3$ as coherent excitations in pump–probe transient reflectivity

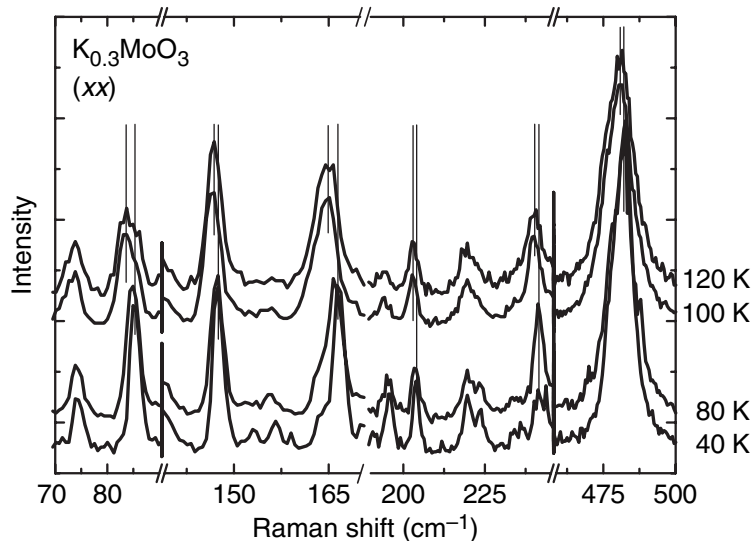


Figure 5. Details of the (xx) polarized Raman spectra of $K_{0.3}MoO_3$ showing a discontinuous energy shift between 80 and 100 K for some of the modes. The spectra have been given an offset for clarity.

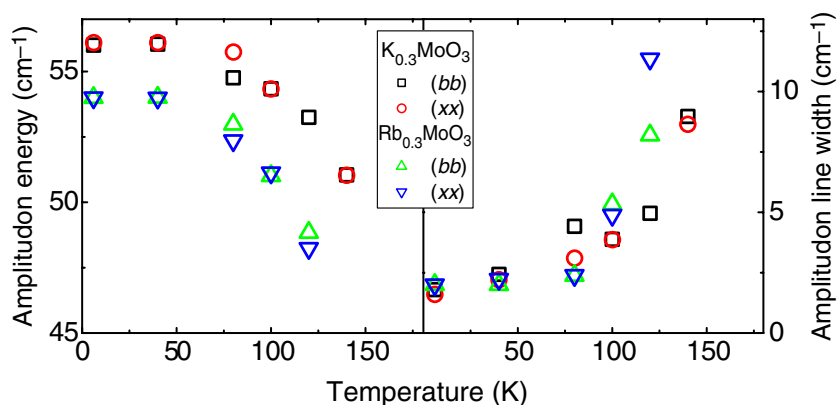


Figure 6. Temperature-dependent energy (left panel) and line width (right panel) of the amplitudon mode in $K_{0.3}MoO_3$ and $Rb_{0.3}MoO_3$.

experiments [29, 30], in addition to coherent phonon excitations [30] at 74 and 85 cm^{-1} also observed in the present data. The amplitudon modes disappear from the spectra already around 150 K. This is due to the strongly overdamped nature of the amplitudon in the vicinity of the phase transition to the metallic state originating from strong fluctuations of the CDW. These fluctuations lead to a diverging line width (see figure 6, right panel), which in turn makes it impossible to observe complete amplitudon softening. The observable amplitudon softening upon approaching the phase transition amounts to only about 10%, as is shown in figure 6 (left panel).

Finally, consider the phonon modes observed in the CDW phase. The phonon modes observed at low temperatures are rather narrow, and often resolution-limited. This is in particular

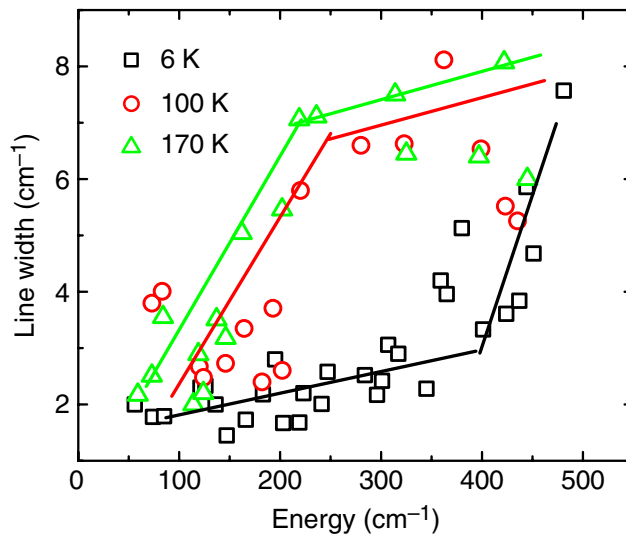


Figure 7. Line width of the phonon modes in $\text{K}_{0.3}\text{MoO}_3$ as a function of their energy for $T = 6100$ and 170 K.

true for the phonons below 400 cm^{-1} . Figure 7 displays the measured line width of the phonons as a function of their frequencies in $\text{K}_{0.3}\text{MoO}_3$ for various temperatures. As can be seen from the figure, at 6 K the line widths of the modes are very narrow up to $\sim 350\text{ cm}^{-1}$. In contrast, the modes above 350 cm^{-1} show a progressive increase in their line width. In other words, there is a sharp onset near 350 cm^{-1} in the behaviour of the line widths. As the temperature is increased, this onset shifts to lower frequencies. A similar behaviour is observed in $\text{Rb}_{0.3}\text{MoO}_3$.

The observed anomalous line broadening hints at a coupling of the phonons to electronic excitations with an energy above $\sim 350\text{ cm}^{-1}$, which, given the temperature dependence, scale with the CDW gap. Since the CDW energy gap in $\text{K}_{0.3}\text{MoO}_3$ is about 900 cm^{-1} , it can not be a coupling to the usual quasi-particle excitations. It has been argued in the literature that a common feature of incommensurate CDW materials is the presence of the so-called midgap states [31]. Therefore the anomalous broadening of the phonons above $\sim 350\text{ cm}^{-1}$ is tentatively assigned to a coupling of the phonons to midgap state excitations.

5. Summary

In summary, we have studied two representatives of the prototypical quasi-1D CDW system, blue bronze, using temperature- and polarization-dependent Raman scattering experiments. The CDW transition leads to the activation of a large number of modes in the low-temperature phase of both the bronzes. The amplitudon mode, found at nearly equal energy in $\text{Rb}_{0.3}\text{MoO}_3$ and $\text{K}_{0.3}\text{MoO}_3$ (there is a 2 cm^{-1} difference between them), shows a rapid exponential broadening upon approaching the phase transition from below, making it impossible to observe a full softening of this mode. The observation of a number of additional modes in the $\text{Rb}_{0.3}\text{MoO}_3$ compound is assigned to the stronger incommensurate modulation in this compound. This conclusion is, however, based on a limited number of low-temperature structural studies, and it would be interesting to perform additional studies to confirm the present interpretation. This also holds for the observed changes in the $\text{K}_{0.3}\text{MoO}_3$ spectra between 80 and 100 K , which

indicate a first-order phase transition. This is in line with the recent discussion of the maximum in the threshold field for CDW conduction which was interpreted as due to an incommensurate–‘commensurate’ phase transition (lock-in transition), where the ‘commensurate’ phase is characterized by commensurate regions separated by mobile discommensurations [32], which by itself is consistent with the presence of midgap states. This transition is not related to the observation of a glass transition in $K_{0.3}MoO_3$ that was recently reported by Starešinić *et al* [33] at $T_g \sim 10$ K, for which no further evidence was found in the present study. Finally, evidence is found for a coupling of the high-frequency phonons to midgap excitations.

Acknowledgments

This work is part of the research programme of the ‘Stichting voor Fundamenteel Onderzoek der Materie (FOM)’, which is financially supported by the ‘Nederlandse Organisatie voor Wetenschappelijk Onderzoek (NWO)’. Financial support by the DFG SPP1073 is gratefully acknowledged.

References

- [1] Peierls R E 1955 *Quantum Theory of Solids* (New York: Oxford University Press)
- [2] Grüner G 1994 *Density Waves in Solids* (Cambridge, MA: Perseus)
- [3] Grüner G 1988 *Rev. Mod. Phys.* **60** 1129
- [4] Tessema G X and Mihaly L 1987 *Phys. Rev. B* **35** 7680
- [5] Zettl A and Grüner G 1982 *Phys. Rev. B* **26** 2298
- [6] Kuzmany H 1998 *Solid State Spectroscopy: An Introduction* (Berlin: Springer)
- [7] Devereaux T P and Hackl R 2007 *Rev. Mod. Phys.* **79** 175
- [8] Travaglini G, Mörke I and Watchter P 1983 *Solid State Commun.* **45** 289
- [9] Hirata T and Ohuchi F S 2001 *Solid State Commun.* **117** 361
- [10] Perlstein J H and Sienko M J 1968 *J. Chem. Phys.* **48** 174
- [11] Becca F, Tarquini M, Grilli M and Castro C D 1996 *Phys. Rev. B* **54** 12443
- [12] Sykora S, Hubsch A, Becker K W, Wellein G and Fehske H 2005 *Phys. Rev. B* **71** 45112
- [13] Nishio S and Kakihana M 2000 *Solid State Commun.* **116** 7
- [14] Ghedira M, Chenavas J, Marezio M and Marcus J 1985 *J. Solid. State Chem.* **57** 300
- [15] Schutte W J and de Boer J L 1993 *Acta Crystallogr. B* **49** 579
- [16] Fleming R M, Schneemeyer L F and Moncton D E 1985 *Phys. Rev. B* **31** 899
- [17] Ramanujacharya K V, Greenblatt M and McCarroll W H 1984 *J. Crystal Growth* **70** 476
- [18] Chua Y T, Stair P C and Wachs I E 2001 *J. Phys. Chem. B* **105** 8600
- [19] Beato P 2005 Synthesis and characterization of realistic molybdenum oxide based model systems in heterogeneous catalysis *PhD Thesis* Technical University of Berlin
- [20] Negishi H, Negishi S, Kuroiwa Y, Sato N and Aoyagi S 2004 *Phys. Rev. B* **69** 064111
- [21] Nishio S and Kakihana M 2001 *Phys. Rev. B* **63** 033104
- [22] Massa N E 1990 *Solid State Commun.* **76** 805
- [23] Wang J, Xiong R, Yi F, Yin D, Ke M, Li C, Liu Z and Shi J 2005 *J. Solid State Chem.* **178** 1440
- [24] Pouget J P, Hennion B, Filippini C E and Sato M 1991 *Phys. Rev. B* **43** 8421
- [25] Tenne D A, Park S, Kampen T U, Das A, Scholz R and Zahn D R T 2000 *Phys. Rev. B* **61** 14564
- [26] Davydov A S 1971 *Theory of Molecular Excitons* (New York: Plenum)
- [27] Fausti D, Nugroho A A, van Loosdrecht P H M, Klimin S A, Popova M N and Bezmaternykh L N 2006 *Phys. Rev. B* **74** 024403

- [28] Currat R and Janssen T 1987 *Solid State Phys.* **41** 201
- [29] Demsar J, Biljakovic K and Mihailovic D 1999 *Phys. Rev. Lett.* **83** 800
- [30] Sagar D M, Tsvetkov A A, Fausti D, van Smaalen S and van Loosdrecht P H M 2007 *J. Phys.: Condens. Matter* **19** 346208
- [31] Nakano M and Machida K 1986 *Phys. Rev. B* **33** 6718
- [32] Yue S, Kuntscher C A, Dressel M, van Smaalen S, Ritter F and Assmus W 2005 Doping effects on the charge-density-wave dynamics in blue bronze *Preprint cond-mat/0501332*
- [33] Starešinić, Hosseini K, Brütting W, Biljakovic K, Riedel E and van Smaalen S 2004 *Phys. Rev. B* **69** 113102